



## Studies of Yttrium Substitution in $\text{PbTiO}_3$ Systems

ABDELHALIM ELBASSET<sup>1,2</sup>, LAMIAE MRHARRAB<sup>2</sup> and SALAHEDINE SAYOURI<sup>2</sup>

<sup>1</sup>LSSC Department of Electrical Engineering, Faculty of Science and Technology (FST),  
Universit Sidi Mohamed Ben Abdellah, Fes, Morocco.

<sup>2</sup>Département de Physique, University Sidi Mohammed Ben Abdellah,  
Faculté des Sciences D-M, B.P.1796, Fès-Atlas Maroc.

\*Corresponding author E-mail: elbasset.abdelhalim@gmail.com

<http://dx.doi.org/10.13005/ojc/330143>

(Received: October 10, 2016; Accepted: December 28, 2016)

### ABSTRACT

Sol gel processed Lead titanate  $\text{PbTiO}_3$  was successfully doped by yttrium (Y) and characterized by X-Ray diffraction (XRD) and Raman spectroscopy. The results obtained showed that Yttrium lead to a sharp decrease in the lattice parameter, c, accompanied by a small increase in a parameter up to 10% yttrium. By cons beyond 10 mol%, these parameters a and c are evolving slightly to converge towards the same value ( $a \approx c$ ). The investigations done by Raman spectroscopy showed that a concentration threshold appears around 10% of Y corresponding to a change in the substitution process in PT sites. it was revealed that substitution of  $\text{Pb}^{2+}$  by  $\text{Y}^{2+}$ , not require the charge compensating, by cons when the rate Y is greater than 10%, the substituted yttrium replaces both  $\text{Pb}^{2+}$  and  $\text{Ti}^{4+}$  in the  $\text{PbTiO}_3$  structure which requires charge compensation.

**Keywords:** Load compensating, Yttrium (Y), Lead titanate  $\text{PbTiO}_3$ .

### INTRODUCTION

Lead titanate ( $\text{PbTiO}_3$  (PT)) a perovskite type compound has a great scientific and technological interest. This compound belongs to the of high performance materials for various types of applications: dielectrics for capacitors, electromechanical converters, infrared detectors, electro optical modulators, memories. The method of preparation of these material plays a very important role in their properties, it can lead to the

improvement of these properties, even the discovery of new things (original). However, suitable suitable PT doping (ion substitution) allows for example to modulate the dielectric constant, the Curie temperature, the relaxation frequency or resonance, for such a given application. In the case of these PT ceramics, disorder metal cations, at site B (Ti) of the perovskite structure  $\text{ABO}_3$  ( $\text{PbTiO}_3$ ), is the common point of all the complex compounds such as  $\text{PZT}^1$ ,  $\text{PZN-PT}^2$ ,  $\text{PMN-PT}^3$ . However for compounds based on  $\text{PbTiO}_3$  with good density and reducing the

fragility and also to study the structural and dielectric properties, many dopants were used (Ca, Co, W, La, Sm, Dy and Mn...) <sup>4-9</sup>.

However, no structural study of Y doped  $\text{PbTiO}_3$  doped Y was presented in the literature. Consequently, this document provides a Raman investigation on the effect of the doping rate (Y) the vibrational modes of  $\text{PbTiO}_3$  powders and its distribution in the PT sites with the study of its influence on the macroscopic symmetry of the mesh. The analysis of the spectra obtained by the Raman spectroscopy shows that the site occupied by the Y depends on its concentration. From the results obtained, we established a model indicating that up to 10% Y,  $\text{Y}^{2+}$  ions integrated site A, whereas beyond of 10% it they may occupied both sites A ( $\text{Pb}^{2+}$ ) and B ( $\text{Ti}^{4+}$ ).

### Synthesis

$\text{Pb}_{1-x}\text{Y}_x\text{TiO}_3$  (PYT) powders with x varying from 0 to 0.3 were obtained by the sol-gel method, a soft chemical route. Accordingly, titanium isopropoxide (99% purity, Aldrich) was dissolved in an aqueous solution of citric acid, to have a colloidal solution of titanium. A stoichiometric amount of ground of titanium was added to the lead acetate,  $\text{Pb}(\text{CH}_3\text{COO})_2 \cdot 3\text{H}_2\text{O}$ , (99% purity, Aldrich).  $\text{Y}(\text{CH}_3\text{COO})_3 \cdot 3\text{H}_2\text{O}$  (99.9% purity, Aldrich) dissolved in nitric acid was used as source of Y and added to the reaction mixture. The mixtures Put under agitation in  $60^\circ\text{C}$  for a few minutes, then were dried at  $80^\circ\text{C}$  for 96 hours. For material crystallization, Every powder

were heat treated at  $650^\circ\text{C}$  for 4 h under oxygen flow in a tube furnace. The formation of the crystalline phase of the sintered samples was analyzed by X-ray diffractometry (XRD) at room temperature using a PANalytical X'Pert Pro diffractometer system with Cu K $\alpha$  radiation from  $15^\circ$  to  $80^\circ$  at  $2\theta$  intervals. A micro Raman spectrometer (Horiba Jobin-Yvon) was used with an excitation source at 532 nm at a power level of 40 mW, providing from the second harmonic line of a Nd:YAG laser, and with a CCD (charge-coupled device) detector. Spectra were recorded at room temperature in the range 50 - 3500  $\text{cm}^{-1}$ .

### RESULTS

XRD spectrum of PT powder (Fig.1) has characteristic peaks of the tetragonal structure of  $\text{PbTiO}_3$  without the presence of secondary phases. The lines of doublets [(001-100), (101-110), (002-200), (201-210) and (112-211)] are characteristic of this phase<sup>10</sup>. For Y doped PT it is always observed peaks indicating the presence of pure perovskite phase. We can also indicate that up to 30 mol %, yttrium is soluble in the PT. However; when the rate of Y increases lines of doublets cited above tend to merge which implies a decreasing quadracity of the unit cell. These figures show as a parameter undergoes an average increase of 4.6% between pure PT and PYT: 10%, then a relatively small increase of 0.4% between 10% and 30% of yttrium. However, the parameter C undergoes a significant decrease (19.1%) between 0% and 10% of Y, then a very slow decay up to 30%. Otherwise, the quadracity

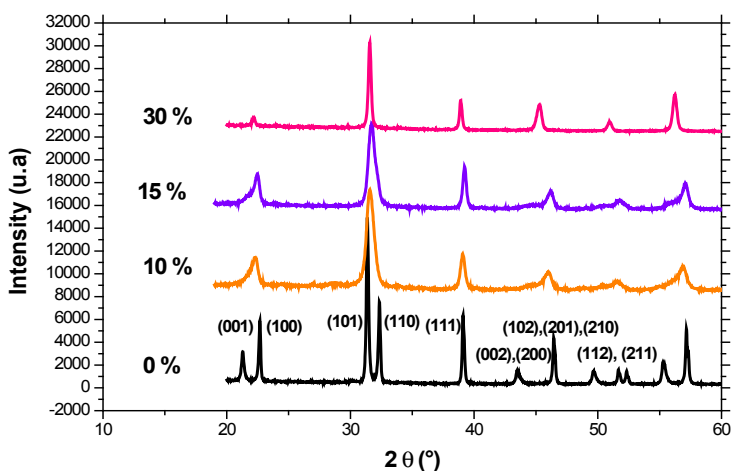


Fig.1: XRD spectra of powder of pure and doped PT

$c/a$  decreases in a brutal way, (6.07%) between 0% and 10% of Y, then an almost linear manner to 30% in Y has a value close to unity (Fig. 2).

We noted that the addition of low concentrations in yttrium (<10%) is accompanied by a significant decrease of the quadracity  $c/a$ . We can interpret this decrease based on the substitution of  $Pb^{2+}$  ions by  $Y^{2+}$  ions. Indeed,  $Y^{2+}$  and  $Pb^{2+}$  have the same valence, which favors the phenomenon of substitution of Pb ions by those of Y in PT matrix. However, the ionic radius of Y,  $r(Y) = 0.9 \text{ \AA}$ , lower than that of Pb, is equal to  $r(Pb)=1.2$ . This difference between ionic radii and electronegativity is responsible for changing the structure of  $PbTiO_3$ . In the case of pure lead titanate, in accordance with the value of Goldsmith tolerance factor ( $t < 1$ ) 11, the structure is quadratic. In other words, the parameter  $c$  is greater than the parameter  $a$  giving more possibilities for mobility of Pb ions along the  $c$ -axis (Figure 3.a). Or when  $Y^{2+}$  ion substitutes  $Pb^{2+}$  ion, the distance Pb-Pb corresponding to the parameter  $c$  is transformed into distance Pb-Y, the  $c$  decreases because the radius of Y is less than that of Pb. Based on this fact and assuming that Y is always placed in the A site (Fig.3.b) we can expect that the increase of Pb ion substitution rates by Y results in a reduction of the distances between the sites A and consequently a decrease in the parameter  $c$ . This is in good agreement with the results we have achieved for dopant concentrations up to 10% of Y from the XRD PYT spectra, the

parameter  $c$  decreases sharply, while the parameter  $a$  undergoes only a small increase of a slowdown in unit cell mesh and therefore an increase in coulombic force in the presence in that direction. However, when the rate of Y increases beyond 10%,  $c$  decreases slightly and tends towards the parameter  $a$  which unlike the parameter  $c$  increases slightly. It shall indicate that within this range the parameters  $a$  and  $c$  virtually no longer change, which allows to assume that part of  $Y^{2+}$  ions started to occupy the site (B of  $ABO_3$ ), Ti radius  $r_{Ti} = 0.69$  and comparable in size to the radius  $r_Y$  of Y. From a structural point of view and considering the Ti-O distance equal to distance Y-O, changing the geometry of octahedra  $BO_6$  should be almost identical in the case of octahedra  $YO_6$  that in the case of octahedra  $TiO_6$ . This suggests a saturation of incorporation on the natural site of the ion  $Pb^{2+}$  (for  $x > 0.1$ ) and incorporation of dopant ions on the B natural site of  $Ti^{4+}$  ions (Figure 3.c). It does not exist in the literature, to our knowledge, information about lead titanate ceramics doped with yttrium allowing us to confirm our model and to make a comparative study with our results. We therefore considered the obtained results with a dopant that is closest to our case study: ion  $Ca^{2+}$  <sup>12-18</sup>. Indeed, the latter possesses the same valence as the Y with an ionic radius  $r_{Ca} = 1 \text{ \AA}$  intermediate between that of the Y and lead.

The interpretation of the results of the analysis of the structural properties of  $PYT:x$ , can therefore be approximated by the results of the

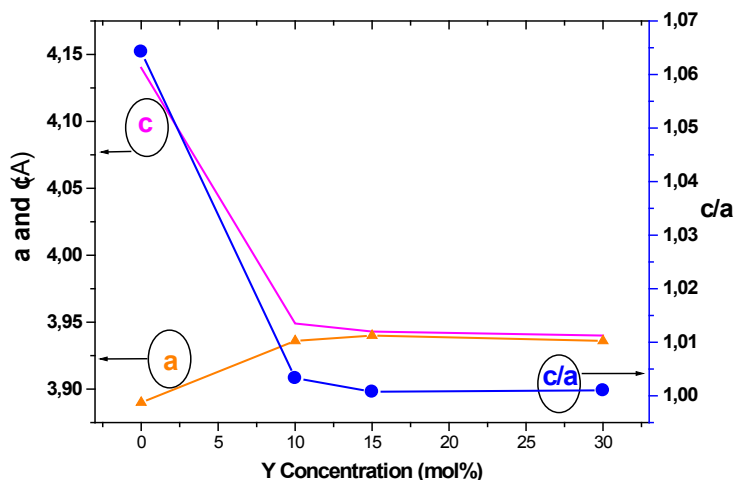


Fig. 2: Evolution of the quadracity  $c/a$  for PYT samples

literature in PCaT:x. Table 1 presents the results of studies of PT doped of different calcium levels prepared by different routes and placed under various forms.

Note that Ca doping reduces the lattice parameter  $c$  and the quadracity  $c/a$ , but the decrease is more significant in PYT:x (table 1)<sup>12-18</sup>. This difference in behavior with the two dopings can be explained by the relative value of the ionic radius of  $\text{Ca}^{2+}$ , which is greater than  $\text{Y}^{2+}$ . Indeed, the quadracity the  $c/a$  of PT:Y decreases faster when replacing  $\text{Pb}^{2+}$  ions by  $\text{Y}^{2+}$  ion, indicating that the quadracity  $c/a$  is strongly correlated to the ionic radius of the dopant. However, note that the lattice parameters are very influenced by the ionic nature of atomic bonds and the physicochemical factors related to the preparation<sup>13, 14</sup>.

Figure 4 shows the Raman spectra of pure and doped PT materials. We can notice that all modes of vibration of pure PT are characteristic of the tetragonal structure. A number of these patterns persist in the Raman spectra of different

compositions. Otherwise, when the concentration of Y increases to 10% (fig. 4) we can observe the disappearance of modes  $\text{E}(\text{LO}_2)$  and  $\text{B1+E}$  and the gradual disappearance of mode  $\text{E}(\text{TO}_1)$ , accompanied by a significant decrease in intensity of the modes  $\text{A1}(\text{TO}_1)$ ,  $\text{E}(\text{TO}_1)$  and  $\text{A1}(\text{TO}_3)$  and an enlargement of the other bands.

This expansion is the result of the disordered character of the phase and these changes can be attributed to the presence of defects created to ensure the electrical neutrality of the unit cell. This result shows that the tetragonal structure of PT seems to disappear for the other samples showing the appearance of a pseudo-cubic phase. The adjustment of the Raman active modes confirms that the frequency and width at half heights modes of PYT:x are sensitive to Y doping. Indeed, Figure 5.a confirms that the frequencies of these modes vary with the concentration of Y. In particular the two modes  $\text{E}(\text{TO}_1)$  and  $\text{A}_1(\text{TO}_1)$  no longer appear on the Raman spectra for the 30% concentration, due to the pseudo cubic structure that these compositions exhibits. Or, we know from the literature<sup>19</sup> that these

**Table 1: Parameters of mesh composed PT:Ca it prepared by different methods and different concentrations of  $\text{Ca}^{2+}$**

% of Ca	a (Å)	c (Å)	c/a	Method	Condition	Refe.
24	3.89	4.04	1.04	Sol gel	Massif	12
40	3.89	3.94	1.01			
50	3.89	3.89	1			
20	3.83	4.03	1.05	Sol gel	Film	15
24	3.86	4.02	1.04			
28	3.89	3.97	1.02			
0	3.884	4.106	1.057	Sol gel	Film	16
10	3.881	4.061	1.046			
20	3.875	4.022	1.038			
20	—	—	1.045	Conventional	Massif	17
40	—	—	1.015	solid state		
50	—	—	1.003	reaction		
0	3.89	4.14	1.0642	Sol gel	Massif	18
1	3.891	4.1386	1.0636			
4	3.8915	4.135	1.0625			
7	3.8919	4.13	1.0611			
10	3.8922	4.127	1.0603			
32	3.893	4.049	1.04			

modes correspond to the vibration of ions at site A (Pb) from the octahedra  $\text{BO}_6$  ( $\text{TiO}_6$ ). The movements associating vibration  $E(\text{TO}_1)$  and  $A_1(\text{TO}_1)$  modes are along the axes a and c, respectively<sup>20</sup>.

When the structure of  $\text{PYT}:x$  changes from tetragonal phase to cubic phase (following the increase in doping) these two Raman modes tend to become inactive. For the mode  $E(\text{TO}_1)$  the change in the position is accompanied by a significant decrease of FWHM for the low concentration ( $x = 0.1$ ) until complete for sample with 30 mol % in Y (Fig. 5). By opposition, the, (FWHM), of the mode

$A_1(\text{TO}_1)$  remains constant and decreases beyond 10% of Y. Following the experimental results and primarily that of the Raman spectroscopy, lead us to consider the charge compensation phenomenon, and equations related to it, necessary to ensure the neutrality of the new structure during the introduction of the dopant. In the pure PT structure, The  $\text{Pb}^{2+}$  ions are at the sites A while  $\text{Ti}^{4+}$  ions occupy the site B.  $\text{Y}^{2+}$  ions for the low levels up to 10% replace the  $\text{Pb}^{2+}$  ions in their sites (A) because they have the same valence. This affects the width at half height and hardens modes  $E(\text{TO}_1)$  and  $A_1(\text{TO}_1)$  with increasing yttrium. More precisely, doping Y induces small

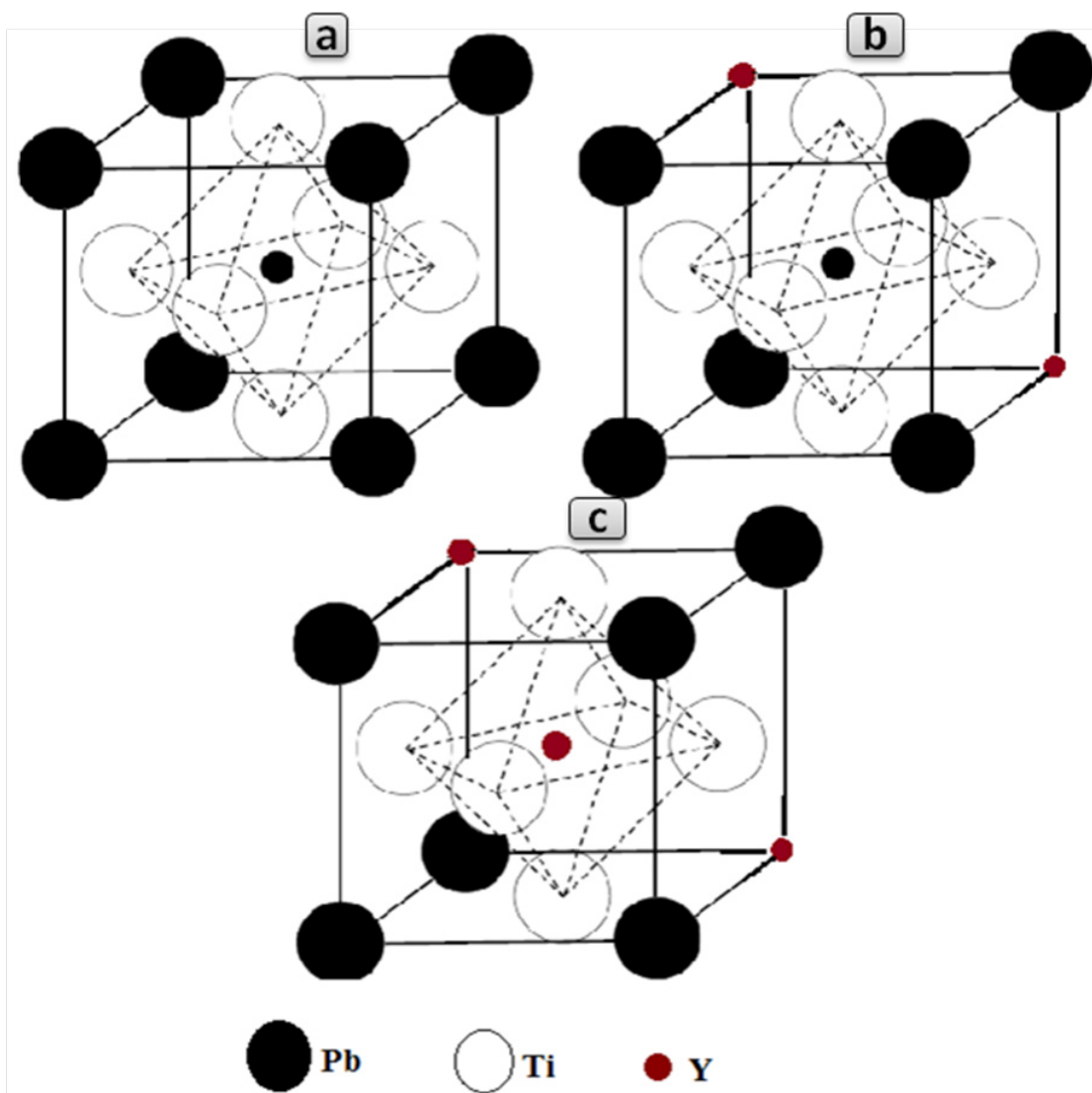


Fig. 3: Diagram of  $\text{PYT}:x$  [(a):  $x = 0\%$ , (b)  $0 < x \leq 10\%$ , and (c):  $x > 10\%$ ] structure

displacements between ions at site A and octahedra  $\text{TiO}_6$ . The octahedra  $\text{TiO}_6$  restrict the displacement of  $\text{Ti}^{4+}$  ions inducing a hardening of soft modes. Substitution in  $\text{PbTiO}_3$  with a divalent ion,  $\text{Y}^{2+}$  sites in the occupied bivalent lead ion  $\text{Pb}^{2+}$  does not require load compensation until the concentration of Y is environ 10%, according to the following chemical formula:



Although this process of substitution does not lead to the creation of the vacant site it induces lattice distortions due to the difference of the ion ray. So, this substitution process involves a change in the stiffness of the cells around the site A and then a change in the frequency of the mode with increasing  $\text{Y}^{2+}$  (figure 4 (a)). When the rate of Y is greater than 10%, a slight decrease in the frequency and the FWHM mode  $\text{A}_1(\text{TO}_1)$  is observed. The Y ions thus reveal an order of the structure that can be attributed to a short structural order. In this concentration range, we concluded that the  $\text{Y}^{2+}$  ions of low atomic radius compared to  $\text{Pb}^{2+}$ , substitute both  $\text{Pb}^{2+}$  and  $\text{Ti}^{4+}$  and therefore incorporate both the A and B sites of the PT structure. Consequently, beyond 10% of Y the substitution of  $\text{Ti}^{4+}$  by  $\text{Y}^{2+}$  requires charge compensation. After several models based on different charge compensation mechanisms, we propose a charge compensation model based on the creation of oxygen deficiencies according to the following formula:



Or x corresponds to the limit concentration of Y 10% and  $\gamma$  is a vacancy on the oxygen site. This solution is the only valid among all the one we studied because it is the only one that corresponds to the evolution of Raman peaks associated sites occupancy of various with ions. Raman spectra of the powder  $\text{Ba}_{0.0975}\text{Sr}_{0.025}\text{TiO}_3$  calcined at various temperatures are shown in Figure 4. Between 200 and 300  $\text{cm}^{-1}$ , there are two modes A ( $\text{LO}_1$ ) and A ( $\text{TO}_2$ ) are respectively 218 and 247  $\text{cm}^{-1}$ , however the increase of the calcination temperature and causes a gradual decrease in the intensity thereof to the appearance of a single broadband 900°C. We observed there also a narrow band with 305  $\text{cm}^{-1}$  associated with the modes B1 and  $\text{E}(\text{TO}_3 + \text{LO}_2)$ , and a wide and asymmetrical strip with 520  $\text{cm}^{-1}$  associated with the modes  $\text{A}_1(\text{TO}_3)$  and  $\text{E}(\text{TO}_4)$  and another wide strip (not very intense) with 720  $\text{cm}^{-1}$  associated with the modes  $\text{A}_1(\text{LO}_3)$  and  $\text{E}(\text{LO}_4)$ .

One notes also the increase in intensity of the mode  $\text{E}(\text{LO}_4)/\text{A}_1(\text{LO}_3)$  by against that of  $\text{E}(\text{TO}_3 + \text{LO}_2) / \text{B1}$  becomes very important. This is closely related to the significant increase in lattice parameter that we showed earlier in Figure 2. This indicates a trend towards the tetragonal phase. Indeed, many researchers agree on the fact that the presence of  $\text{E}(\text{TO}_3)$  to 305  $\text{cm}^{-1}$  mode comes from idle F2U of the cubic phase, is a characteristic of the tetragonal phase of the BT structure<sup>10-11</sup>. And that the decrease

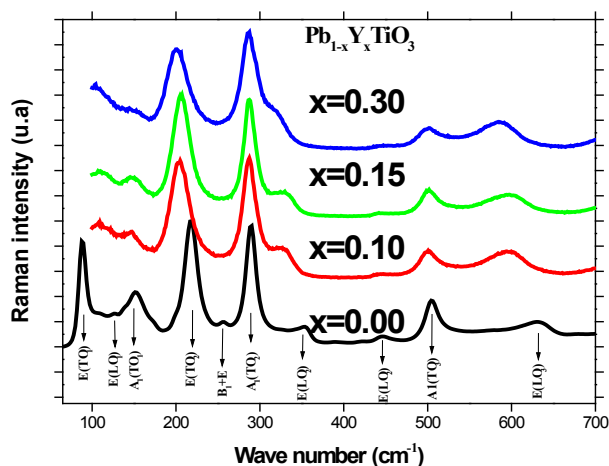


Fig. 4: Raman spectra of pure and doped PT materials

of the number of Raman bands is a consequence of an increase in the lattice symmetry<sup>9,12</sup>.

Those are the consequence of shift of frequencies of the Raman modes. Also note the

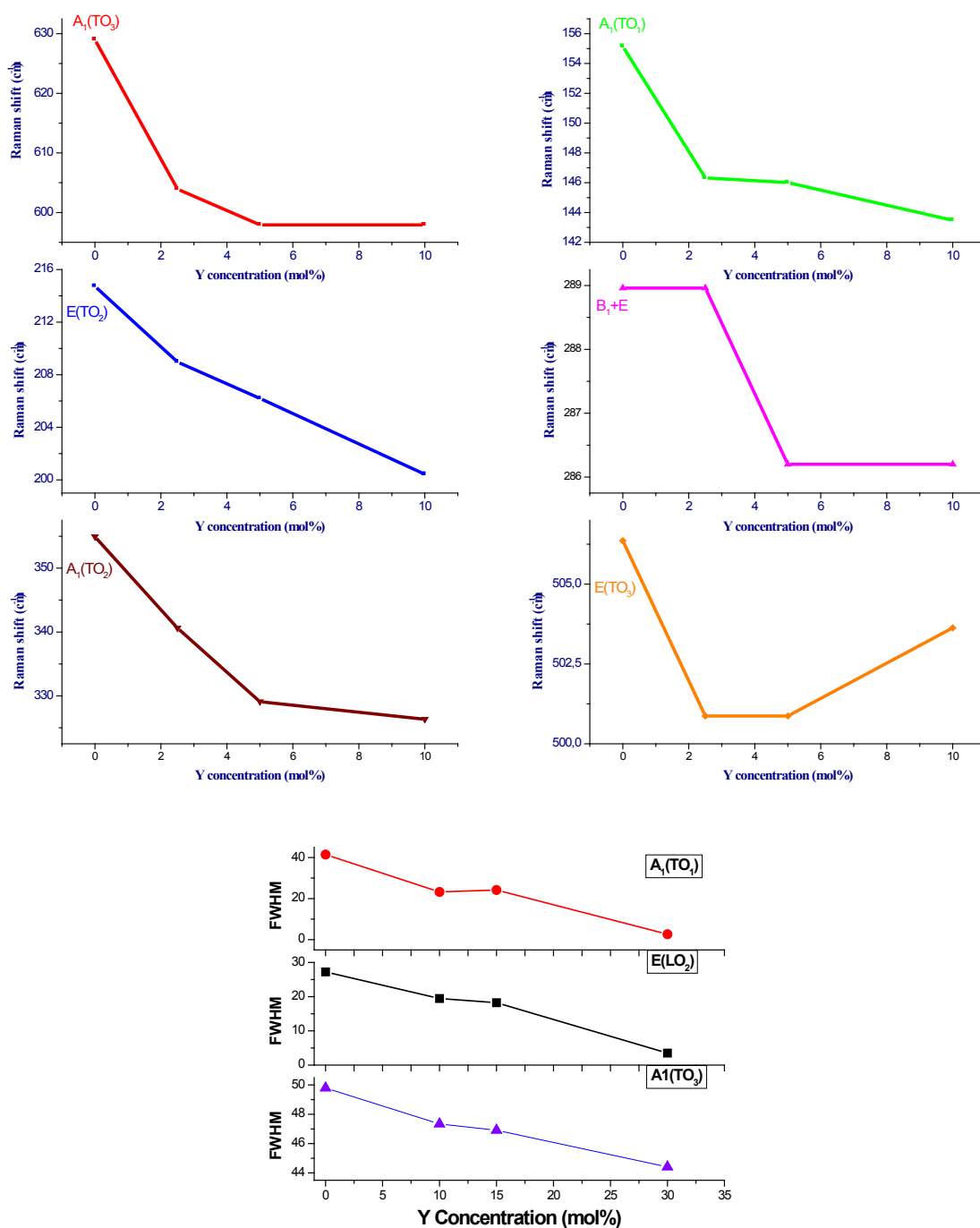


Fig. 5: Positions and FWHM of Raman modes for different concentrations in Y in PTYx

presence of new bands at 117 and 804  $\text{cm}^{-1}$ , which have never been mentioned in the literature, note that this band does not appear in the 900°C spectrum, may be it is closely related with the secondary phase  $\text{BaCO}_3$ . This is in analogy with the observation by X-ray diffraction.

### CONCLUSION

The sol-gel method permits the synthesis of  $(\text{Pb}_{1-x}\text{Y}_x)\text{TiO}_3$  powders for concentrations up to 30 mol %. X-ray diffraction analysis showed that all powders crystallized in the perovskite phase, it was verified that the increase in the yttrium

concentration favors the PT phase transition from tetragonal to pseudo-cubic by a sharp decrease in the lattice parameter  $c$ . For 30 % the disappearance of the  $E(\text{LO}_2)$ ,  $B_1+E$  and  $E(\text{TO}_1)$  modes clearly demonstrates this tendency. with the characterization by Raman spectroscopy we founded a hypothesis by considering the charge compensation phenomenon. The substitution of the divalent lead ion  $\text{Pb}^{2+}$  in  $\text{PbTiO}_3$  by a divalent ion  $\text{Y}^{2+}$  does not require charge compensation until the concentration of Y is about 10%. Above this threshold, the substituted yttrium has both the ions  $\text{Pb}^{2+}$  and  $\text{Ti}^{4+}$  PT structure which requires a charge compensation according to the formula indicated above.

### REFERENCES

- Noheda, B.; Cox, D.E.; Shirane, G.; Guo, R.; Jones, B.; *Cross, L.E. Physical Review*. **2001**, *63*, .014103, 1, 141031.
- Renault, A-E.; Dammak, H.; Calvarin, G.; Pham Thi M.; and Gaucher, P. *Japanease Journal of Applied Physiscs*, **2002**, 41, 1.
- Ye, Z. G.; Noheda, B.. Dong, M.; Cox, D.; and Shirane, G. *Physical Review*. **2001**, *B. 64*, 18,184114.
- Paik, D.S.; Prasadarao, A.V.; Komarneni, S. *Mater. Lett.* **1997**, *97*, 2-3,
- Calzada, M.L.; Sirera, R.; Ricote, J.; Pardo, L. *J. Mater. Chem.* **1998**, *8*, 111, Kellati, M.; Thèse de la faculté des sciences Dhar Mehraz, Fes, **2002**.
- Renault, A-E. ; Dammak, H. ; Gaucher, P. ; Pham Thi, M. and Calvarin, G. IEEE, ISAF Proceeding, (XIIIth International Symposium on the Applications of Ferroelectrics, **2002**. 28 1(Nara, Japon))
- Castañeda-Guzmán, R.; x Villagrán-Muniz, R.; . Saniger-Blesa, J. M ; Pérez-Ruiz, S. J.; and Pérez-Martínez, O. *Appl. Phys. Lett.* , **2000**. *77*, 3087
- Venkateswarlu, P. ; Bharadwaja, S.S.N. ; Krupanidhi, S.B. *Thin Solid Films*. **2001**. *389*,1-2, 84
- Li, H. ; Tang, X. ; Li, Q. ; Liu, Y. ; Tang, Z. ; Zhang, Y. ; Mo, D. ; *Solid State Commun.***2000**. *114*, 6, 347.
- Shirane, G. ; Pepinsky, R. ; and Frazer, B. C. ; *Acta Crystallogr.* **1956**. *9*, 131
- Kallati, M. ; El moudden, N. ; Kaal, A. ; Elghazouali A. and Sayouri, S. ; *Annales de chimie des Sciences des Materiaux*. **2002**. *27*, 1, 43
- Calzada, M. L. ; Bretos, I. ; Jiménez, R. ; Ricote, L. Mendiola, *J. Thin Solid Films*. **2004**. *450*, 211
- Carmona, F. ; Calzada, M. L.; Roman, E.; Sirera, R.; Mendiola, J. **1996**. *Thin Solid Films*, 279, 70
- Mendiola, J. ; Ramos, P. ; Calzada, M. L. ; *Phys. J. Chem. Solid*. **1998**. *59*, 9, 1571
- Chopra, S.; Sharma, S.; Goel, T. C.; *Mendiratta, R. G. Solid State communication*. **2003**. *127*, 299
- Tang, X.G.; Zhou, Q.F.; Zhang, J.X. *Thin Solid Films*. **2000**. *375*, 1-2, 159
- Ganesh, R.; Goo, E.; *Am. J. Ceram. Soc.* **1997**. (3), 653
- Elmsbahi, A.; Kherbeche, A.; Kadira, Lh.; Sayouri, S.; Lotfi, M.; Zenkouare, M.; Elaatmani, M.; *Cata. J. Mat. Env.***2003**. *11*, 51
- Freire, J.D.; Katiyar, R.S. *Phys.* **1988**. *Rev.*, *B* *37*, 2074
- Dobal, P.S.; Majumder, S.B.; Bhaskar S.; and Katiyar, R.S. *J. Raman Spectrosc.* **1999**. *30*, 7, 567.